*International Journal of Computational Vision and Biomechanics*
*Vol. 5 No. 2 (July-December, 2019)*

MUK PUBLICATIONS
Open Access Publisher

# Computational Modelling of Ligaments at Non-physiological Situations

**B. Calvo, E. Peña, M.A. Martínez and M. Doblaré**

*Group of Structural Mechanics and Material Modelling, Aragon Institute of Engineering Research (I3A)*
*University of Zaragoza (Spain)*

*Submitted: 15th January 2019* *Revised: 29th March 2019* *Accepted: 30th July 2019*

*A proper understanding of joints biomechanics is essential to improve the prevention and treatment of their disorders and injuries. Despite the many investigations developed in this field, the exact mechanical behavior of the different human joints and the causes of many of their injuries are not completely known yet. Computational models provide therefore a powerful tool for the study of joint function, prosthesis design, and the effects of joint reconstruction. Reliability of these models strongly depends on a precise geometrical reconstruction and on an accurate mathematical description of the behavior of the biological tissues involved, and their interactions with the surrounding environment.*
*The objective of the paper is to describe constitutive models for addressing the computational modelling of ligaments under non-physiological loads. Hyperelastic, viscoelastic, initial strains and damage models are presented to describe the mechanical behavior of ligaments in these situations. In order to show the performance of the framework presented herein, a complex 3D numerical application to ligament mechanics of the anterior cruciate ligament is presented. Results show that the model is able to capture the typical stress-strain behavior observed in ligaments at non-physiological situations and seem to confirm the soundness of the proposed framework.*

*Keyword: Computational biomechanics, ligaments, hyperelasticity, viscoelasticity, damage, finite element method*
*Computational modeling of ligaments at non-physiological situations B. Calvo, E. Peña, M.A. Martínez and M. Doblaré*

## 1. INTRODUCTION

Biomechanics is defined as the development, extension and application of mechanics for the purpose of the better understanding physiology and pathophysiology, as well as, the diagnosis and treatment of disease and injury. That is, the overall goal of biomechanics is, and must remain, the general improvement of the human condition [9].

Finite element (FE) method offer, the potential to predict quantities that are difficult or impossible to measure experimentally. In particular, FE method offers the ability to predict spatial and temporal variations in stress, strain, contact area and forces. The FE method also provides a standardized framework for parametric studies, such as evaluation of multiple clinical treatments. A computational analysis may predict possible stress distributions for different geometries and kinematics, provide a basis for evaluation of surgical procedures, and aid in medical education and virtual surgery. The need for such a tool has many uses in the areas of injury assessment and surgery planning [27]. However, the construction of accurate and useful models requires integration of the mechanics concepts, experimental results, and material models and the reliability of these models strongly depends on an appropriate geometrical reconstruction and on an accurate mathematical descriptions of the behavior of the biological tissues involved, and their interactions with the surrounding environment [16].

The construction of an accurate constitutive model is difficult because ligaments are non-linear, anisotropic, inhomogeneous, viscoelastic, and undergo large deformations [27]. In addition, ligaments are usually exposed to a complex distribution of “in vivo” residual stresses as a consequence of the continuous growth, remodelling, damage and viscoelastic strains that they suffer along their whole life [15]. Ligaments, also, exhibit simultaneously elastic and viscous material behavior. This behavior can arise from the fluid flow inside the tissue, from the inherent viscoelasticity of the solid phase, or from viscous interactions between the tissue phases [10]. Furthermore, non-physiological loads drive soft tissue to damage that may induce a strong reduction of the stiffness. In order to obtain a realistic and complete material model under non-physiological situations, elastic behavior, initial strains, viscoelasticity and damage may be coupled to account inelastic features.

With all the above in mind, the objective of the paper is to describe constitutive models for addressing the computational modelling of ligaments under non-physiological situations using FE method, differentiating between elastic, viscoelastic, initial strains and damage of the ligaments and applications. The paper is organized as follows. Section 2 describes the basic structure of the ligaments. In Section 3 the constitutive models for ligaments, hyperelasticity, initial strains, viscoelasticty and damage are presented. The application to some examples is presented in section 4. Finally, section 5 includes some concluding remarks.

## 2. STRUCTURE AND PROPERTIES OF LIGAMENTS

Tendons and ligaments are soft tissues composed of closely packed, parallel collagen fiber bundles oriented to provide

motion and stability to the musculoskeletal system. Under macroscopic examination, ground substance is observed in the interfibrillar spaces. Although ligaments are considered as composite material consisting of a ground substance matrix reinforced by collagen and elastin, collagen is the primary component that resists the tensile stress in ligaments.

The tensile modulus of the ligament depends on the collagen fibril density, fibril orientation and the amount of collagen cross-linking. When this tissue is tested in tension, the collagen fibrils are aligned and stretched along the axis of loading. For small deformations, when the tensile stress in the specimen is relatively small, a nonlinear toe-region is seen in the stress-strain curve, due to realignment of the collagen fibres, rather than stretching of these fibers. For larger deformations, and after realignment, the collagen fibrils are stretched and therefore generate a larger tensile stress due to the intrinsic stiffness of the collagen fibrils themselves. Due to this phenomenon, the tensile stiffness of ligaments is highly strain dependent (see Fig. 1).

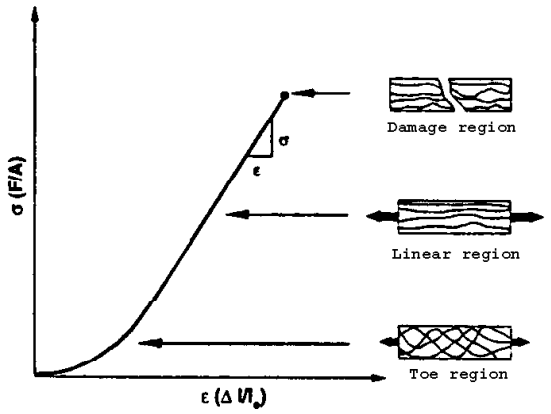


**Figure 1: Schematic diagram of of a uniaxial tensile test where fibers orient in the direction of the load as it increases.**

## 3. CONSTITUTIVE MODELS FOR LIGAMENTS

### 3.1 Continuum Description of the Elastic Behavior

Consider a continuum body with reference configuration $\mathbf{\Omega}_0$ at the initial reference time $t = 0$. Then, an assumed motion $\chi$ maps this configuration to the current configuration $\mathbf{\Omega}$ at each time $t$. Hence, a point $\mathbf{X} \in \mathbf{\Omega}_0$ transforms to a point $\mathbf{x} \in \mathbf{\Omega}$, where $\mathbf{X}$ and $\mathbf{x}$ define the respective positions of a particle in the reference and current configurations relative to a fixed set of axes. The direction of a fiber at a point $\mathbf{X} \in \mathbf{\Omega}_0$ is defined by a unit vector field $\mathbf{m}_0(\mathbf{X})$, $|\mathbf{m}_0| = 1$. It is usually assumed that, under deformation, the fiber moves with the material points of the continuum body. Therefore, the stretch $\lambda$ of the fiber defined as the ratio between its lengths at the deformed and reference configurations can be expressed as

$$\lambda \mathbf{m}(\mathbf{x},t) = \mathbf{F}(\mathbf{X},t)\mathbf{m}_0(\mathbf{X}); \lambda^2 = \mathbf{m}_0 \cdot \mathbf{F}^T\mathbf{F} \cdot \mathbf{m}_0 = \mathbf{m}_0 \cdot \mathbf{C}\mathbf{m}_0 \quad (1)$$

where $\mathbf{m}$ is the unit vector of the fiber in the deformed configuration, $\mathbf{F} = \frac{\mathbf{dx}}{\mathbf{dX}}$ and $\mathbf{C} = \mathbf{F}^T\mathbf{F}$ are the standard deformation gradient and the corresponding right Cauchy-Green strain measure.

A multiplicative decomposition of $\mathbf{F} = J^{\frac{1}{3}}\overline{\mathbf{F}}$ and $\mathbf{C} = J^{\frac{2}{3}}\overline{\mathbf{C}}$ into *volume-changing (dilational)* and *volume-preserving (distortional)* parts is usually established as in [5] and [23].

To characterize isothermal processes, we postulate the existence of a unique decoupled representation of the strain-energy density function $\mathbf{\Psi}$ [23]. Because of the directional dependence on the deformation, we require that the function $\mathbf{\Psi}$ explicitly depends on both the right Cauchy-Green tensor $\mathbf{C}$ and the fibers direction $\mathbf{m}_0$ in the reference configuration. Since the sign of $\mathbf{m}_0$ is not significant, $\mathbf{\Psi}$ must be an even function of $\mathbf{m}_0$ and so it may be expressed by $\Psi = \Psi(\mathbf{C}, \mathbf{M})$ where $\mathbf{M} = \mathbf{m}_0 \otimes \mathbf{m}_0$ is the structural tensor [25]. Based on the kinematic description, the free energy can be written in decoupled form as

$$\Psi(\mathbf{C}, \mathbf{m}_0) = \Psi_{vol}(J) + \overline{\Psi}(\overline{\mathbf{C}}, \mathbf{M}) = \Psi_{vol}(J) + \overline{\Psi}(\overline{I}_1(\overline{\mathbf{C}}), \overline{I}_2(\overline{\mathbf{C}}), \overline{I}_4(\overline{\mathbf{C}}, \mathbf{m}_0), \overline{I}_5(\overline{\mathbf{C}}, \mathbf{m}_0)) \quad (2)$$

where $\Psi_{vol}(J)$ and $\overline{\Psi}(\overline{\mathbf{C}}, \mathbf{M})$ are given scalar-valued functions of $J$, $\overline{\mathbf{C}}$ and $\mathbf{m}_0$ respectively that describe the volumetric and isochoric responses of the material [8], $\overline{I}_1$ and $\overline{I}_2$ the first two modified strain invariants of the symmetric modified Cauchy-Green tensor $\overline{\mathbf{C}}$ (Note that $I_3 = J$ and $\overline{I}_3 = 1$). Finally, the pseudo-invariants $\overline{I}_4, \overline{I}_5$ characterize the constitutive response of the fibers [25]:

$$\overline{I}_4 = \mathbf{C} : \mathbf{M}, \overline{I}_5 = \mathbf{C}^2 : \mathbf{M} \quad (3)$$

While the invariant $\overline{I}_4$ has a clear physical sense, the square of the stretch $\lambda$ in the fiber direction, the influence of $\overline{I}_5$ is difficult to evaluate due to the high correlation among the invariants. For this reason and the lack of sufficient experimental data it is usual not to include this invariant in the definition of $\mathbf{\Psi}$ [25].

We now define the constitutive equation for compressible hyperelastic materials in the standard form

$$\mathbf{S} = 2\frac{\partial \Psi(\mathbf{C}, \mathbf{M})}{\partial \mathbf{C}} = \mathbf{S}_{vol} + \overline{\mathbf{S}} = Jp\mathbf{C}^{-1} + \overline{\mathbf{S}} \quad (4)$$

where the second Piola-Kirchhoff stress $\mathbf{S}$ consists of a purely volumetric contribution $\mathbf{S}_{vol}$ and a purely isochoric one $\overline{\mathbf{S}}$ and $p$ is the hydrostatic pressure. The associated decoupled elasticity tensor may be written as

$$C = C_{vol} + C_{iso} = 2\frac{\partial \mathbf{S}_{vol}}{\partial \mathbf{C}} + 2\frac{\partial \overline{\mathbf{S}}}{\partial \mathbf{C}} \quad (5)$$

Using the push-forward operator we obtain the Cauchy stress tensor $\sigma = J^{-1}\chi_*(\mathbf{S})$ and the elasticity tensor in the spatial description $_{\mathbb{C}} = J^{-1}\chi_*(C)$. For a more detailed derivation of the material and spatial elasticity tensors for completely incompressible or compressible fibred

hyperelastic materials and their explicit expressions, see i.e. [8] or [25].

### 3.2 Enforcing Initial Strains of Ligaments

Initial strains are a consequence of the continuous growth, remodelling, damage and viscoelastic strains that suffer living materials along their whole life. Initial strains can be relieved by selective cutting of the living tissue and removal of its internal constraints. In ligaments of diarthrodial joints, initial stretches provide joint stability even in a relatively unloaded joint configuration [7]. Typical residual strains are approximately 3-5% in these ligaments.

In order to describe the current deformation state of a solid, including the effect of initial deformations, three different configurations are usually defined: a) the stress-free state ($\mathbf{\Omega}_{sf}$), b) the reference state in which the material is unloaded ($\mathbf{\Omega}_0$) and c) the current deformed state ($\mathbf{\Omega}$).

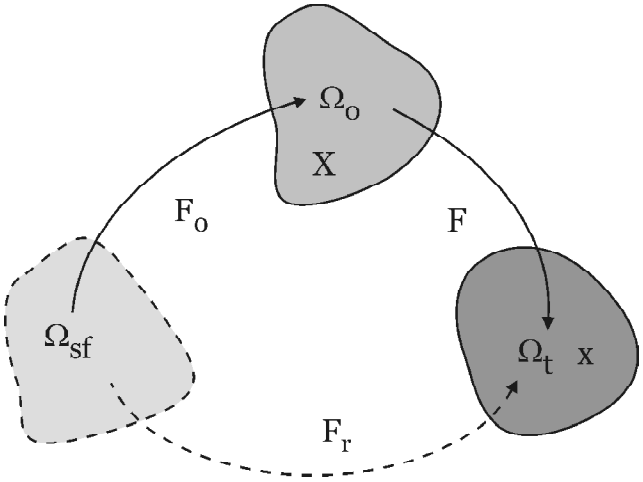


**Figure 2: Multiplicative decomposition of the total deformation gradient where $\mathbf{\Omega}_{sf}$ denotes the stress free state, $\mathbf{\Omega}_0$ the reference state and $\mathbf{\Omega}$ the current configuration [15].**

It is assumed that the total deformation gradient tensor corresponding to the current state ($\mathbf{F}_r$) admits a multiplicative decomposition [15] such as:

$$\mathbf{F}_r = \mathbf{F}\mathbf{F}_0 \tag{6}$$

The initial stress in the reference state, $\sigma_0$, is defined for hyperelastic materials in the standard form, by the strain-energy density function $\Psi_{\Omega_{sf}}$. Note that this function is always referred to the stress-free state $\mathbf{\Omega}_{sf}$ while $\boldsymbol{\sigma}_0$ are true stresses in the reference load-free configuration. Then

$$\sigma_0 = \frac{2}{J_0}\chi_*\left[\frac{\partial \Psi_{\Omega_{sf}}(\mathbf{C})}{\partial \mathbf{C}}|_{\mathbf{C}=\mathbf{C}_0}\right] = \frac{2}{J_0}\mathbf{F}_0\left[\frac{\partial \Psi_{\Omega_{sf}}(\mathbf{C})}{\partial \mathbf{C}}|_{\mathbf{C}=\mathbf{C}_0}\right]\mathbf{F}_0^T \tag{7}$$

with $\chi_*$ the push-forward associated to $\mathbf{F}_0$ and $\mathbf{C}_0 = \mathbf{F}_0^T\mathbf{F}_0$.

In the same way, it is possible to define the total stresses corresponding to the current state $\sigma_r$ in the standard form by using the strain-energy density function $\Psi_{\Omega_{sf}}$ through $\mathbf{F}_r$.

$$\sigma_r = \frac{2}{J_r}\chi_{*r}\left[\frac{\partial \Psi_{\Omega_{sf}}(\mathbf{C})}{\partial \mathbf{C}}|_{\mathbf{C}=\mathbf{C}_r}\right] = \frac{2}{J_r}\mathbf{F}_r\left[\frac{\partial \Psi_{\Omega_{sf}}(\mathbf{C})}{\partial \mathbf{C}}|_{\mathbf{C}=\mathbf{C}_r}\right]\mathbf{F}_r^T \tag{8}$$

with $J_r = J_0 J$ and $\mathbf{C}_r = \mathbf{F}_r^T\mathbf{F}_r$.

Finally, the elasticity tensor in the material description

$$\mathbb{C} = 4\frac{\partial^2 \Psi_{\Omega_{sf}}(\mathbf{C})}{\partial \mathbf{C}\partial \mathbf{C}}|_{\mathbf{C}=\mathbf{C}_r} \tag{9}$$

As noted, $\mathbf{F}_0$ is difficult to determine from experiments. In the case of ligaments and tendons, Gardiner *et al.* [6] proposed a relatively easy form to measure length variations along the fiber direction at different points, that is, $\mathbf{F}_0$ corresponds to an axial stretch $\lambda_0$ along the fiber direction $\mathbf{a}_0$ in the reference state $\Omega_0$. Using the incompressibility condition, $\mathbf{F}_0$ can be written in a coordinate system (*) where the fiber direction $\mathbf{a}_0$ is aligned with the $X_1$ axis as:

$$\left[\mathbf{F}_0^*\right] = \begin{bmatrix} \lambda_0 & 0 & 0 \\ 0 & \frac{1}{\sqrt{\lambda_0}} & 0 \\ 0 & 0 & \frac{1}{\sqrt{\lambda_0}} \end{bmatrix} \tag{10}$$

To introduce initial strains into the finite element formulation, it is necessary to specify $\mathbf{F}_0$ pointwise within the finite element mesh. An equilibrium step is firstly applied with zero forces with the constitutive behaviour defined by $\Psi_{\Omega_{sf}}$ in order to obtain a balanced, although not fully compatible configuration. A second load step will result in the deformation gradient $\mathbf{F}$ that balances the externally applied forces.

### 3.3 Continuum Description of the Viscoelastic Behavior of Ligaments

In order to describe viscoelastic effects we consider the finite-strain anisotropic viscoelastic constitutive behaviour proposed by [14]. They apply the concept of internal variables [22] and postulate the existence of an uncoupled free energy function $\Psi(\mathbf{C},\mathbf{Q})$ of the form

$$\Psi(\mathbf{C},\mathbf{M},\mathbf{Q}_{ij}) = \Psi_{vol}^0(J) + \overline{\Psi}_0 - \frac{1}{2}\sum_{i=1}^{N}\sum_{k=m,f_1}(\overline{\mathbf{C}}:\mathbf{Q}_{ik}) + \Xi(\sum_{i=1}^{N}\sum_{k=m,f_1}\mathbf{Q}_{ik}) \tag{11}$$

where $\mathbf{\Omega}_{ik}$ may be interpreted as non-equilibrium stresses, in the sense of non-equilibrium thermodynamics, and remain unaltered under superposed spatial rigid body motions. $\mathbf{\Omega}_{im}$ are the isotropic contribution due to the matrix material associated to $I_1$ and $I_2$ invariants and $\mathbf{Q}if$ is the anisotropic contribution due to the fibres associated to $I_4$, $I_5$ invariants [14].

Standard arguments based on the Clausius-Duhem inequality $D_{int} = -\dot{\Psi} + \frac{1}{2}\mathbf{S}:\dot{\mathbf{C}} \geq 0$, lead to the representation

$$\mathbf{S} = 2\frac{\partial \Psi(\mathbf{C},\mathbf{M},\mathbf{Q}_{ik})}{\partial \mathbf{C}} = Jp\mathbf{C}^{-1} + J^{-\frac{2}{3}}DEV[2\frac{\partial \bar{\Psi}^0(\bar{\mathbf{C}},\mathbf{M})}{\partial \bar{\mathbf{C}}} - \sum_{i=1}^{N}\mathbf{Q}_{ik}] = \mathbf{S}_{vol} + \bar{\mathbf{S}}^0 - J^{-\frac{2}{3}}\sum_{i=1}^{n} DEV[\mathbf{Q}_{ik}] \tag{12}$$

where *DEV* is the deviator operator in the material description [24].

Based on previous studies [19, 21, 26], the ligament is assumed to have a Kelvin-Voigt-type viscoelastic constitutive behaviour. The nonequilibrium second Piola Kirchhof stresses in (12), $\mathbf{Q}_{ik}$, are assumed to be governed by a set of linear rate equations

$$\dot{\mathbf{Q}}_{ik} + \frac{1}{\tau_{ik}}\mathbf{Q}_{ik} = \frac{\gamma_{ik}}{\tau_{ik}} DEV[2\frac{\partial \bar{\Psi}^0_k(\bar{\mathbf{C}},\mathbf{M})}{\partial \bar{\mathbf{C}}}] \qquad \lim_{t\to-\infty}\mathbf{Q}_{ik} = 0 \tag{13}$$

where $\gamma_{ik} \in [0,1]$ are free energy factors associated with relaxation times $\tau_{ik} > 0$.

The evolution equations (13) are linear and, therefore, explicitly lead to the following convolution representation

$$\mathbf{Q}_{ik}(t) = \frac{\gamma_{ik}}{\tau_{ik}}\int_{-\infty}^{t} \exp[\frac{-(t-s)}{\tau_{ik}}] DEV[2\frac{\partial \bar{\Psi}^0_k}{\partial \bar{\mathbf{C}}}]ds \tag{14}$$

Algoritmically, the constitutive model is appealing since equation (13) can be evaluated via a simple recursion relation which was originally developed for finite strains by [22]. In particular, if the material state is known at a time $t_n$ and the deformation is known at a time $t_{n+1} = t_n + \Delta t$ with $\Delta t > 0$, we may write

$$\mathbf{S}_{n+1} = J_{n+1}p_{n+1}\mathbf{C}^{-1}_{n+1} + J^{-\frac{2}{3}}_{n+1}\sum_{k=m,f_1}[(1-\sum_{i=1}^{N}\gamma_{ik})\bar{\mathbf{S}}^0_{(k)n+1}]) + \\ + J^{-\frac{2}{3}}_{n+1}\sum_{i=1}^{N}[\gamma_{ik}\{DEV[\mathbf{H}^{(ik)}_{n+1}]\}] \tag{15}$$

where $\mathbf{H}^{(ik)}_{n+1}$ are internal algorithmic history variables defined by

$$\mathbf{H}^{(ik)}_{n+1} = \exp[\frac{-\Delta t_n}{\tau_{ik}}]\mathbf{H}^{(ik)}_n + \exp[\frac{-\Delta t_n}{2\tau_{ij}}]\{\bar{\mathbf{S}}^0_{(k)n+1} - \bar{\mathbf{S}}^0_{(k)n}\} \tag{16}$$

where the subscripts *n* and *n* + 1 denote quantities evaluated at times $t_n$ and $t_{n+1}$ [22,14].

The iterative Newton procedure to solve a nonlinear finite element problem requires the determination of the consistent tangent material operator. This can be derived analytically for the given material equation (5). The symmetric algorithmic material tensor which is expressed as [22]

$$\mathbb{C}_{n+1} = \mathbb{C}^0_{vol(n+1)} + \sum_{k=m,f_1}[(1-\gamma_k+\nu_k)\bar{\mathbb{C}}^0_{(k)n+1} + \\ -\frac{2}{3}J^{-\frac{4}{3}}_{n+1}\sum_{i=1}^{N}\gamma_{ik}\{DEV[\tilde{\mathbf{H}}^{(ik)}_n]\otimes\bar{\mathbf{C}}^{-1}_{n+1} + \bar{\mathbf{C}}^{-1}_{n+1}\otimes DEV[\tilde{\mathbf{H}}^{(ik)}_n] - \\ -(\tilde{\mathbf{H}}^{(ik)}_n : \bar{\mathbf{C}})(\mathbb{I}^{-1}_{\mathbf{C}_{n+1}} - \frac{1}{3}\bar{\mathbf{C}}^{-1}_{n+1}\otimes\bar{\mathbf{C}}^{-1}_{n+1})\}] \tag{17}$$

with

$$\tilde{\mathbf{H}}^{(ik)}_n = \exp[\frac{-\Delta t_n}{\tau_{ij}}]\mathbf{H}^{(ik)}_n - \exp[\frac{-\Delta t_n}{2\tau_{ij}}]\bar{\mathbf{S}}^{0(j)}_n \tag{18}$$

$$\mathbf{H}^{(ik)}_{n+1} = \tilde{\mathbf{H}}^{(ik)}_n + \exp[\frac{-\Delta t_n}{2\tau_{ij}}]\bar{\mathbf{S}}^{0(j)}_{n+1} \tag{19}$$

### 3.4 On Modeling of Damage Process of Ligaments

In order to reproduce the damage process in ligaments, we consider the directional damage model proposed by Calvo *et al.* [3]. The damage phenomenon is assumed to affect only the isochoric elastic part of the deformation, as proposed by Simo [22]. The free energy density can be written in a decoupled form, such as

$$\Psi(\mathbf{C},\mathbf{M},D_m,D_f) = \Psi_{vol}(J) + (1-D_m)\bar{\Psi}^m_0(\bar{\mathbf{C}}) + (1-D_f)\bar{\Psi}^f_0(\bar{\mathbf{C}},\mathbf{M},\mathbf{N}) \tag{20}$$

where $\mathbf{M}$ is the structural tensor, $\Psi_{vol}(J)$ is a strictly convex function (with the minimum at $J = 1$) which describes the volumetric elastic response, $\bar{\Psi}^m_0$ denotes the isochoric effective strain energy density of the undamaged material, which describes the elastic response of the matrix, and $\bar{\Psi}^f_0$ denotes the isochoric effective strain energy of the undamage material, which describes the isochoric elastic response of the fibers. The factors $(1–D_m)$ and $(1–D_f)$ are known as the reduction factors [22], where the internal variables $D_m \in [0,1]$ and $D_f \in [0,1]$ are normalized scalars referred to as the damage variables for the matrix and fibers respectively.

As a particularization of the Clausius-Planck inequality we obtain

$$\mathbf{S} = \mathbf{S}_{vol} + (1-D_m)\bar{\mathbf{S}}^m_0 + (1-D_f)\bar{\mathbf{S}}^f_0 \tag{21}$$

The evolution of the damage parameters $D_m$ and $D_f$ is characterized by an irreversible equation of evolution as follows. We define $\Xi^m_s, \Xi^f_s$ by the expression [22]

$$\Xi^m_s = \sqrt{2\bar{\Psi}^m_0(\bar{\mathbf{C}}(s))} \quad and \quad \Xi^f_s = \sqrt{2\bar{\Psi}^f_0(\bar{\mathbf{C}}(s))} \tag{22}$$

where $\bar{\mathbf{C}}(s)$ is the modified right Cauchy-Green tensor at time s. Now, let $\Xi^m_t, \Xi^f_t$ be the maximum values of $\Xi^m_s, \Xi^f_s$ over the past history up to current time $t$ that is [22]

$$\Xi^m_t = \max_{s\in(-\infty,t)}\sqrt{2\bar{\Psi}^m_0(\bar{\mathbf{C}}(s))} \quad and \quad \Xi^f_t = \max_{s\in(-\infty,t)}\sqrt{2\bar{\Psi}^f_0(\bar{\mathbf{C}}(s))} \tag{23}$$

We define a damage criterion for the ground substance or matrix in the strain space by the condition that, at any time *t* of the loading process, the following expression is fulfilled [22]

$$\phi_m(\mathbf{C}(t),\Xi^m_t) = \sqrt{2\bar{\Psi}^m_0(\bar{\mathbf{C}}(t))} - \Xi^m_t \le 0 \tag{24}$$

The symmetric algorithmic material tensor which is expressed as

$$\mathbf{C}_{n+1} = \mathbf{C}^0_{vol(n+1)} + \sum_{k=m,f_1} [(1-D_{(k)n+1})\bar{\mathbf{C}}^0_{(k)n+1} - \bar{S}_{(k)n+1}] \quad (25)$$

where

$$\bar{\mathbb{S}}_{(k)n+1} = \begin{cases} \bar{g}'_{(k)n+1}\,\bar{S}^0_{(k)n+1} \otimes \bar{S}^0_{(k)n+1} & \text{if } \phi = 0 \text{ and } \mathbf{N}_m : \dot{\mathbf{C}} > 0 \\ 0 & \text{otherwise} \end{cases}$$

## 4. NUMERICAL EXAMPLES

In order to show the performance of the framework presented herein, some examples are included. The most used isotropically transverse model for ligaments is the early proposed by [29]. However with this model, we can not express the strain energy function in an analytical form. So, the particular form of the deviatoric functions $\bar{\Psi}^m_0$ and $\bar{\Psi}^f_0$ used herein are the proposed by [11]

$$\bar{\Psi}^0_m = C_1(\bar{I}_1 - 3)$$

$$\bar{\Psi}^0_f = \frac{C_3}{2C_4}(\exp^{C_4(\bar{I}_4-1)} - C_4(\bar{I}_4 - 1) - 1) \quad (27)$$

Finally, the volumetric part of the strain energy function is always stated as $\Psi_{vol} = \frac{1}{D}\ln J^2$ [8].

### 4.1 Anterior Cruciate Ligament under Different Strain Rates

Viscoelasticity of ligaments has been clearly demonstrated in creep and stress relaxations tests [17, 18, 19, 28]. There are, however, some variabilities in the findings of different studies performed to evaluate the change in ligament material properties with increasing loading rate [4, 17]. The strain-rate during injury is very important regarding the magnitude of the lesion. Therefore, the stress-strain behavior of the ligament is an essential factor.

To illustrate the performance of the visco-hyperelastic behaviour of ligaments and the importance of the strain-rates during their movement, a model of the human anterior cruciate ligament (ACL) was constructed to simulate its behavior under an anterior tibial displacement, see Fig. 4.a. The surface geometries of femur and tibia were reconstructed from a set of Computer Tomography (CT) images, while for the ACL, MRI (Magnetic Resonance Images) were used [13]. Two different strain rates were applied: low (0.012 $\%S^{-1}$) and high ($50\%S^{-1}$) that correspond to physiological and non-physiological strain-rates.

The elastic and viscoelastic parameters for the human ACL were fitted from published experimental data [17] and are shown in Table 1 and Figure 3. Ligaments were attached to bone. The motion of each bone was controlled by the six degrees of freedom of its reference node. In the analyses, tibia remained fixed. The position at full extension served as the initial reference configuration. An anterior load of 134 N was applied to the femur. In this example we did not consider initial strains [15].

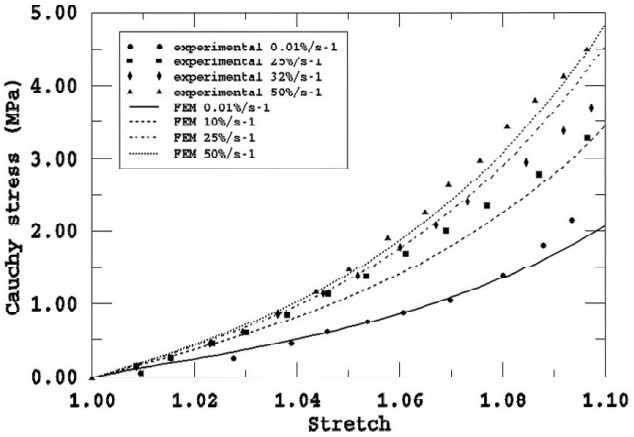


**Figure 3: Experimental results obtained by [17] and theoretical stress-strain curves at different rates of elongation for the human ACL**

**Table 1**
**ACL elastic, viscoelastic and damage material parameters (MPa)**

| | | | | | |
|---|---|---|---|---|---|
| $C_1$ | $C_2$ | $C_3$ | $C_4$ | D | |
| 1 | 0.0 | 0.4 | 8.1019 | 8.8e-3 | |
| $\gamma_m$ | $\tau_m$ | $\gamma_f$ | $\tau_f$ | | |
| 0.31 | 0.15 | 0.69 | 5 | | |
| $\psi^m_{min}$ | $\psi^m_{max}$ | $\beta^m$ | $\psi^f_{min}$ | $\psi^f_{max}$ | $\beta^f$ |
| 0.2946 | 0.4399 | 0.120 | 0.9427 | 1.4086 | 0.1538 |

Maximal principal stress distributions in ACL at $0.012\%S^{-1}$ and $50\%S^{-1}$ of strain rates are presented in Figure 4. The maximal principal stress is located in the central part of the ligament. The maximal principal stress of 7.27 MPa obtained in the central region for the higher load rate is due to the stiffening effect induced by high load rates. Under physiological strain-rates the maximal principal stress of 4.36 MPa is far from the ultimate stress.

### 4.2 Damage of Human Anterior Cruciate Ligament

The anterior cruciate (ACL) ligament is the most frequent totally disrupted of all the knee ligaments. Sports (sky, basketball, soccer) and traffic accidents are the most important causes of ligament injury. Studies of ligament cutting and measurements of tissue load have shown that ACL provides a primary restraint to anterior-posterior and flexion movement and a secondary restraint to external-internal rotation. The purpose of this simulation is to demonstrate the applicability of the model to simulate the structural behavior of soft biological tissues. We reproduce in a human ACL, the experiment developed by [12] in a monkey ACL. That study was performed to determine the viscoelastic behavior of ligaments at different loading rates, such as those associated with sports-related trauma.

The previous human model of the ACL was used to test slow and fast conditions at displacement rates of 0.08467 mm/s and 8.467 mm/s. The elastic, viscoelastic and damage parameters for the human ACL were fitted from published experimental data [1,17] and are shown in Table 1. The fitted curve is shown in Figure 5.

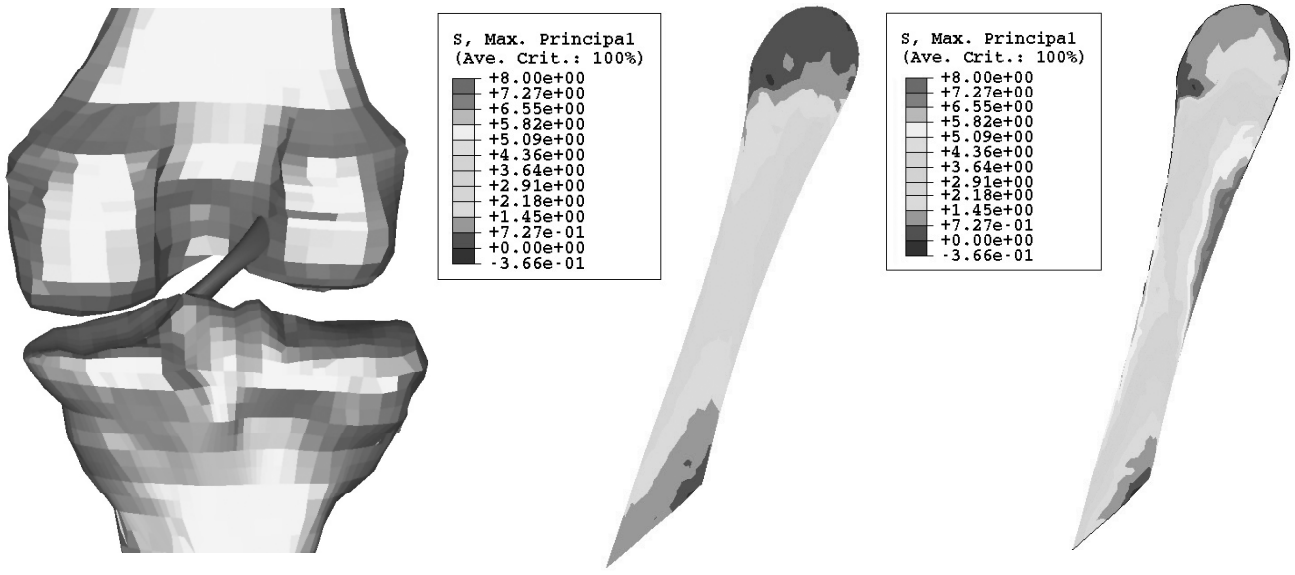


(a) [Finite element model] (b) [0.012 $\%s^{-1}$] (c) [50 $\%s^{-1}$]

**Figure 4: Finite element model of the human ACL and maximal principal stress at low and high strain rates (MPa).**

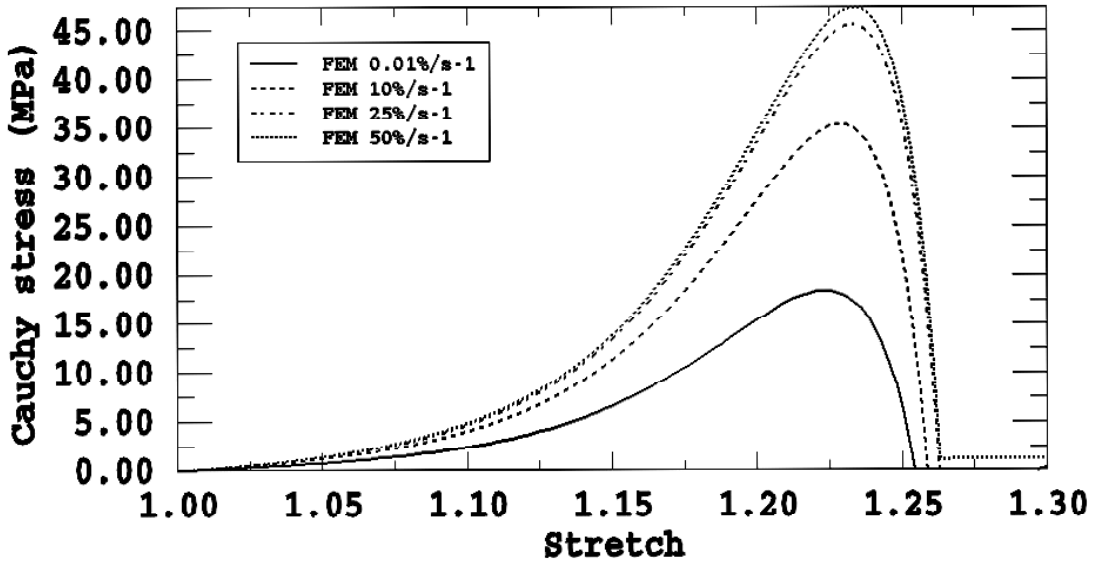


**Figure 5: Stress-strain response of the human ACL at different displacement rates.**

Damage distributions in matrix and fibres at 0.08467 mm/s and 8.467 mm/s of displacement rates are presented in Figures 6 and 7. Due to limitations of the model, we consider failure of the ACL when damage reached a value of 0.55 in both matrix or fibres. We can observe the effect of the strain rate into the damage behavior. At 8.467 mm/s of displacement rate, damage in fibres was much lower (0.34) than at 0.08467 mm/s (0.56). On the contrary, damage in matrix at 8.467 mm/s (0.26) was much higher than at 0.08467 mm/s (0.20). [12] observed that during the failure process, the ligament grossly appears intact while the load is approximately 80 %. The peak values appeared in the ligament substance as has been also reported in previous experimental studies [12]. This is in agreement with the computational results obtained herein due to the damage processes in the matrix substance is lower than in the fibers.

In Table 2 the results are separated according to the strain rate. The overall difference in strength properties at two deformation rates is shown, the load needed until failure at high strain rate is higher than at low strain rate as has been also reported in previous experimental studies [12].

**Table 2**
**Strain Rate Results by Strain Rate**

| *Strain rate* | *Maximun load (N)* | *Strain to failure* |
|---|---|---|
| Fast | 94.88 | 0.41 |
| Slow | 45.1 | 0.4 |

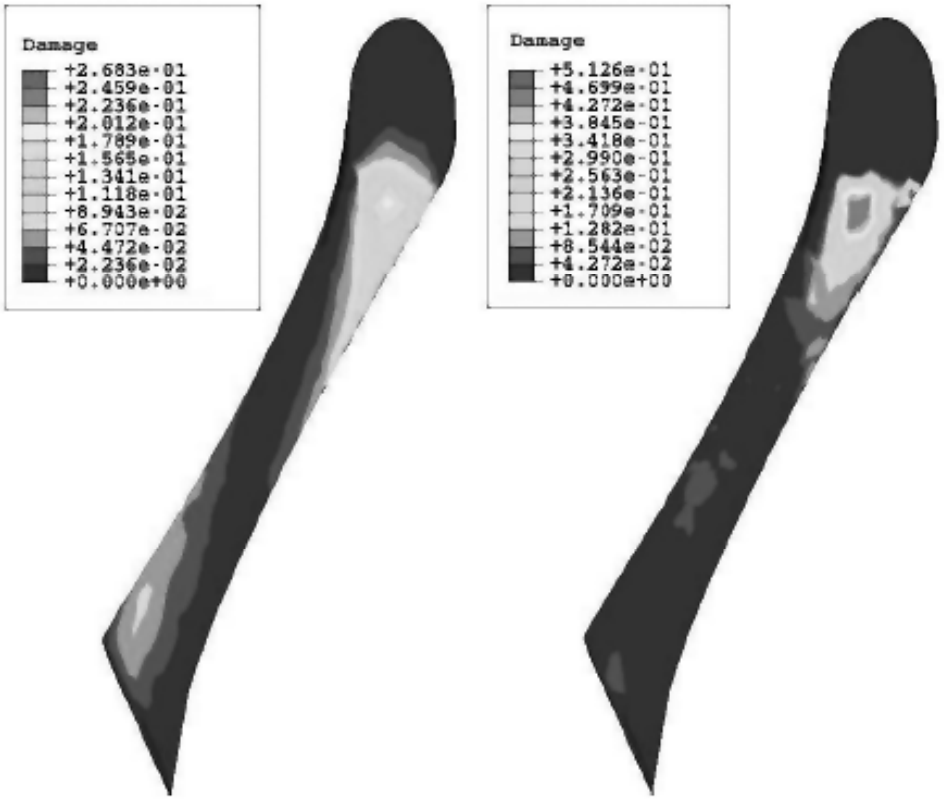


(a) [Matrix damage] (b) [Fibre damage]

**Figure 6: Damage in a human ACL at 0.08467 mm/s**

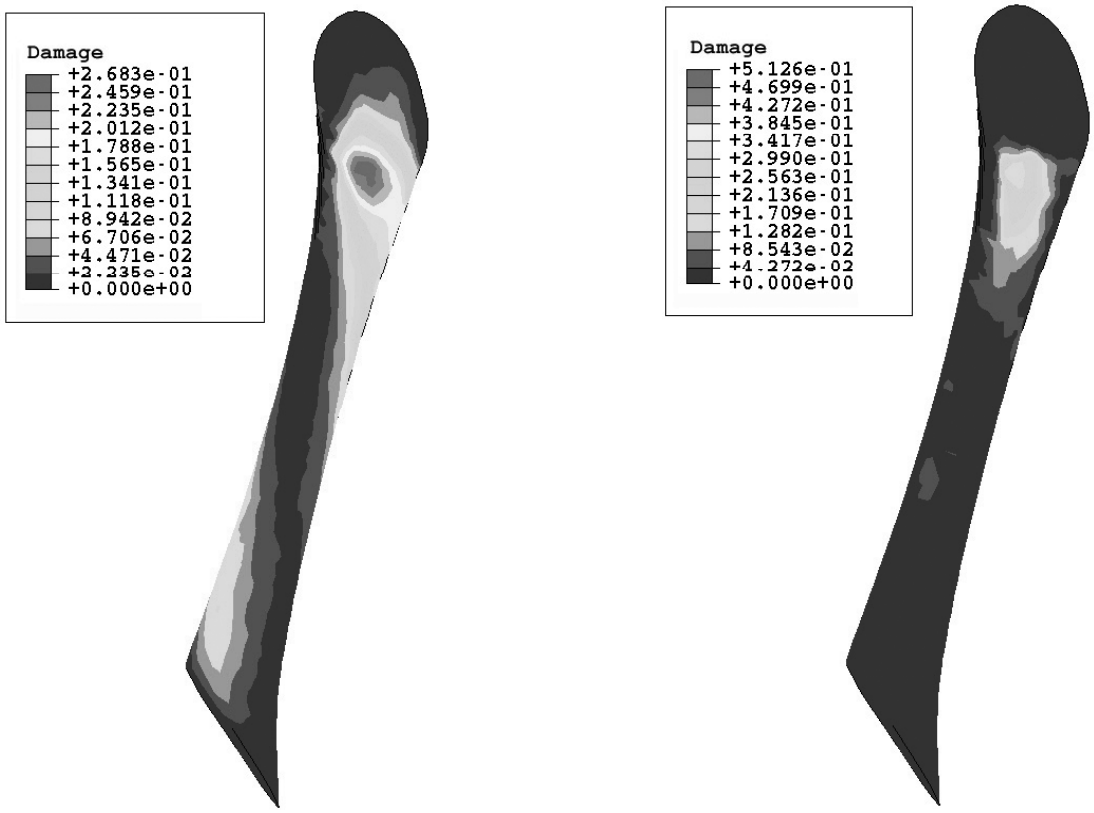


(a) [Matrix damage] (b) [Fibre damage]

**Figure 7: Damage in a human ACL at 8.467 mm/s**

## 5. DISCUSSION

In this work, we have presented constitutive models that have been used to represent ligaments under non physiological situations. The ultimate goal of these modelling efforts is to improve the clinical diagnosis and treatment of different injuries and disorders of diarthrodial joints. This paper presents visco-hyperelastic and damage models to study the strain softening time-dependent behavior of ligaments. The research question addressed in the paper is to assess whether, in the framework of phenomenological models, a time-dependent constitutive damage model with viscoelastic properties different for matrix and reinforcing fibres can predict different experimental evidences in this type of materials [2,20]. From numerical point of view, a general procedure for the simulation of finite strain problems involving dissipative fibred materials has been described in detail. Emphasis has been placed on the numerical treatment of the proposed formulation in the context of the finite element method and particular attention has been paid to the derivation of the corresponding tangent tensor, essential for the solution of the implicit finite element equations.

In order to show the performance of the framework presented herein, a complex 3D numerical application to ACL ligament mechanics is presented. Results show that the model is able to capture the typical stress-strain behavior observed in ligaments at non-physiological situations and predict the damage ligament regions that has been reported in previous experimental studies [12].

### 6. ACKNOWLEDGEMENTS

The authors gratefully acknowledge the support of the Spanish Education and Science Ministry (CYCIT DPI2004-07410-C03-01 and FIS2005-05020-C03-03) and the Spanish Ministry of Health (FIS PI06-0446).

### REFERENCES

[1] Arnoux, P., P-Chabrand, Jean, M., Bonnoit, J. (2002). A visco-hyperelastic with damage for the knee ligaments under dynamic constraints. *Comp Meth in Biomech and Biomedical Eng*. 5, 167–174.

[2] Bonifasi-Lista, C., Lake, S., Small, M., Weiss, J. (2005). Viscoelastoc properties of the human medial collateral ligament under longitudinal, transverse and shear loading. *J. Orthopaed Res*. 23, 67–76.

[3] Calvo, B., Peña, E., Martínez, M., Doblaré, M. (2006). An uncoupled directional damage model for fibered biological soft tissues. Formulation and computational aspects. *Int J. Numer Meth Engng*. 69, 2036–2057.

[4] Danto, M. I., Woo, S. (1993). The mechanical properties of skeletally mature rabbit anterior cruciate ligament and patellar tendon over range of strain rates. Cursive 11, 58–67.

[5] Flory, P. J. (1961). Thermodynamic relations for high elastic materials. *Transaction of the Faraday Societety* 57, 829–838.

[6] Gardiner, J., Weiss, J. (2003). Subjet-specific finite element analysis of the human medial collateral ligament during valgus knee loading. *J. Orthopaed Res*. 21, 1098–1106.

[7] Gardiner, J., Weiss, J., Rosenberg, T. (2001). Strain in the human medial collateral ligament during valgus lading of the knee. *Clin Orthop Relat R* 391, 266–274.

[8] Holzapfel, G. A. (2000). Nonlinear Solid Mechanics. Wiley, New York.

[9] Humphrey, J. D. (2002). Continuum biomechanics of soft biological tissues. *Proc R. Soc Lond A* 175, 1–44.

[10] Mak, A. (1986). The apparent viscoelastic behaviour of articular cartilage. The contributions from the intrinsic matrix viscoelastocity and intersticial fluid flows. *ASME J. Biomech Engng*. 108, 123–130.

[11] Natali, A., Pavan, P., Carniel, E., Luisiano, M., Taglialavoro, G. (2005). Anisotropic elasto-damage constitutive model for the biomechanical analysis of tendons. *Med. Eng. Phys*. 27, 209–214.

[12] Noyes, F., DeLucas, J., Torvik, P. (1974). Biomechanics of anterior cruciate ligament failure: an analysis of strain-rate sensitivity and mechanisms of failure in primates. *J. Bone Joint Surg* 56(A), 236–253.

[13] Peña, E., Calvo, B., Martinez, M., Doblaré, M. (2006a). A three-dimensional finite element analysis of the combined behavior of ligaments and menisci in the healthy human knee joint. *J. Biomech* 39(9), 1686–1701.

[14] Peña, E., Calvo, B., Martínez, M. A., Doblaré, M. (2007a). An anisotropic visco-hyperelastic model for ligaments at finite strains: Formulation and computational aspects. *Int. J. Solids Struct* 44, 760–778.

[15] Peña, E., Calvo, M. A. M. B., Doblaré, M. (2006b). On the numerical treatment of initial strains in soft biological tissues. *Int. J. Numer Meth Engng*. 68, 836–860.

[16] Peña, E., del Palomar, A. P., Calvo, B., Martínez, M., Doblaré, M. (2007b). Computational modelling of diarthrodial joints. Physiological, pathological and pos-surgery simulations. *Arch Comput Method Eng*. 14(1), 1–54.

[17] Pioletti, D., Rakotomanana, L., Benvenuti, J.-F., Leyvraz, P.-F. (1998). Viscoelastic constitutive law in large deformations: application to human knee ligaments and tendons. *J. Biomech* 31, 753–757.

[18] Provenzano, P., Lakes, R., Corr, D., Vanderby, R. (2002). Application of nonlinear viscoelastic models to describe ligament behavior. *Biomech Model Mechanobiol* 1, 45–47.

[19] Puxkandl, R., Zizak, I., Paris, O., Tesch, W., Bernstorff, S., Purslow, P., Fratzl1, P. (2002). Viscoelastic properties of collagen: synchrotron radiation investigations and structural model. Cursive 357, 191–197.

[20] Quapp, K., Weiss, J. (1998). Material characterization of human medial collateral ligament. *ASME J. Biomech Eng*. 120, 757–763.

[21] Sasaki, N., Odajima, S. (1996). Stress-strain curve and Young´s modulus of a collagen molecule as determined by X-ray diffraction technique. *J. Biomech* 29, 655–658.

[22] Simo, J. (1987). On a fully three-dimensional finite-strain viscoelastic damage model: Formulation and computational aspects. *Comput Methods Appl. Mech Engrg* 60, 153–173.

[23] Simo, J., Taylor, R. (1991). Quasi-Incompresible Finite Elasticity in Principal Stretches. Continuum Basis and Numerical Algorithms. *Comput Methods Appl. Mech. Engrg.* 85, 273–310.

[24] Simo, J. C., Hughes, T. (1998). Computational Inelasticity. Springer-Verlag, New York.

[25] Spencer, A. J. M. (1954). Theory of Invariants. In: Continuum Physics. Academic Press, New York, pp. 239–253.

[26] Vita, R. D., Slaughter, W. (2006). A structural constitutive model for the strain rate-dependent behavior of anterior cruciate ligaments. *Int J. Solids Struct*. 43, 1561–1570.

[27] Weiss, J., Gardiner, J. C. (2001). Computational modelling of ligament mechanics. *Crit Rev. Biomed Eng*. 29, 1–70.

[28] Weiss, J., Gardiner, J. C., Bonifasi-Lista, C. (2002). Ligament material behavior is nonlinear, viscoelastic and rate-independent under shear loading. *J. Biomech*. 35, 943–950.

[29] Weiss, J., Maker, B., S.Govindjee (1996). Finite element implementation of incompressible, transversely isotropic hyperelasticity. *Comput Methods Appl. Mech. Engrg*. 135, 107–128.